

Biomechanical Behaviors of Implant-Supported Zirconia Restorations Cemented to Novel Screw-Retained Abutment Systems: A Three-Dimensional Finite Element Analysis Study

Yeni Vida Tutuculu Abutment Sistemlerine Simante Edilen İmplant Destekli Zirkonya Restorasyonların Biyomekanik Davranışları: Üç Boyutlu Sonlu Elemanlar Analiz Çalışması

^{id} Necati KALELİ^a, ^{id} Çağrı URAL^b

^aİstanbul Medeniyet University Faculty of Dentistry, Department of Dentistry, İstanbul, TURKEY

^bOndokuz Mayıs University Faculty of Dentistry, Department of Prosthodontics, Samsun, TURKEY

ABSTRACT Objective: The purpose of this study was to evaluate the biomechanical behaviors of non-engaging titanium base abutments (N-TiBA) bonded to three-unit zirconia restorations in terms of stress distribution in implants and prosthetic components. **Material and Methods:** Three-dimensional (3D) models of a tissue-level and bone-level implant systems and their screw-retained abutments (SRA) and N-TiBA were created. A bone block representing the maxillary right posterior region was created, and the implants were placed in the first premolar and first molar areas. Six different three-unit implant-supported fixed dental prostheses (I-FDPs) models were created: tissue-level implant, N-TiBA, 6 mm crown height (TL6); tissue-level implant, N-TiBA, 10 mm crown height (TL10); bone-level implant, SRA, 6 mm crown height (SR6); bone-level implant, SRA, 10 mm crown height (SR10); bone-level implant, N-TiBA, 6 mm crown height (BL6); bone-level implant, N-TiBA, 10 mm crown height (BL10). The restoration material was determined as monolithic zirconia. In each model, equal vertical (200 N) and oblique (100 N) loads were applied to each tooth simultaneously. The stress distribution in the restoration, implant, abutments, and basal screws was evaluated through the von Mises stress analysis. **Results:** The TL6 and TL10 exhibited higher von Mises stress values in the implants and lower von Mises stress values in the abutments than in the other FEA models. The increase in the crown height resulted in higher stress values under oblique loading compared to vertical loading. **Conclusion:** The non-engaging connection type and crown height affected the stress distribution in the implant and prosthetic components.

Keywords: Non-engaging connection; screw-retained restoration; titanium base abutment

ÖZET Amaç: Bu çalışmanın amacı, üç üyeli zirkonya restorasyonlara simante edilen non-engaging titanyum baz abutmentlerin (N-TiBA) biyomekanik davranışlarını, implant ve protez bileşenlerinde stres dağılımı açısından değerlendirmektir. **Gereç ve Yöntemler:** Doku seviyesi ve kemik seviyesi implant sistemlerine ait vida tutuculu abutmentler (SRA) ve N-TiBA'ların üç boyutlu modellemeleri yapıldı. Sağ maksiller posterior bölgeyi temsil eden bir kemik bloğu oluşturuldu ve implantlar birinci premolar ve birinci molar bölgelerine yerleştirildi. Altı farklı üç üyeli implant üstü sabit parsiyel protez (I-FDP) modeli oluşturuldu: doku seviyesi implant, N-TiBA, 6 mm kron yüksekliği (TL6); doku seviyesi implant, N-TiBA, 10 mm kron yüksekliği (TL10); kemik seviyesi implant, SRA, 6 mm kron yüksekliği (SR6); kemik seviyesi implant, SRA, 10 mm kron yüksekliği (SR10); kemik seviyesi implant, N-TiBA, 6 mm kron yüksekliği (BL6); kemik seviyesi implant, N-TiBA, 10 mm kron yüksekliği (BL10). Restorasyon malzemesi monolitik zirkonya olarak belirlenmiştir. Her modelde, her dişe aynı anda eşit dikey (200 N) ve oblik (100 N) yük uygulandı. Restorasyon, implant, abutmentler ve bazal vidalardaki stres dağılımı von Mises stres analizi ile değerlendirildi. **Bulgular:** TL6 ve TL10 modellemelerinde, implantlarda daha yüksek von Mises stres değerleri gözlenirken ve abutmentlerde daha düşük von Mises stres değerleri gözlemlendi. Kron yüksekliğindeki artış, dikey yüklemeye kıyasla eğik yüklemeye altında daha yüksek stres değerlerine neden oldu. **Sonuç:** Non-engaging bağlantı tipi ve kron yüksekliği, implant ve protez bileşenlerde stres dağılımını etkiledi.

Anahtar Kelimeler: Non-engaging bağlantı; vida tutuculu restorasyon; titanyum baz abutment

Correspondence: Necati KALELİ

İstanbul Medeniyet University Faculty of Dentistry, Department of Dentistry, İstanbul, TURKEY/TÜRKİYE

E-mail: necati_kaleli@hotmail.com



Peer review under responsibility of Türkiye Klinikleri Journal of Dental Sciences.

Received: 05 Apr 2019

Received in revised form: 21 May 2019

Accepted: 22 May 2019

Available online: 13 Jun 2019

2146-8966 / Copyright © 2020 by Türkiye Klinikleri. This is an open access article under the CC BY-NC-ND license (<http://creativecommons.org/licenses/by-nc-nd/4.0/>).

The restoration of missing teeth with implant-supported prosthesis has become a common treatment modality in clinical dentistry.¹ Implant-supported restorations can be either cement-retained or screw-retained, depending on relevant clinical and technical issues.² Both approaches have their advantages and disadvantages.³ Cement-retained restorations stand out as an esthetic solution where the implant angulations are unfavorable and the fabrication stages are more straightforward.⁴ However, excess cement remnants may lead to undesirable complications, such as peri-implantitis.^{5,6} Furthermore, they are highly challenging to remove without damage in case of technical complications.^{3,6} Screw-retained restorations require a technically precise manufacturing process, and the implant placement should be driven prosthetically to provide ideal position of screw access holes.² Nevertheless, screw-retained restorations are more reliable where the interocclusal space is insufficient, and they can be easily removed when hygiene maintenance or repair are required.^{2,4} Therefore, implant-supported restorations as partial or full-arch fixed dental prostheses (FDPs) are recommended to be screw-retained.³

Several restorative materials are used in fabricating multiple-unit implant-supported fixed dental prostheses (I-FDPs).⁷ Metal-ceramic restorations have been considered the “gold standard” for many years and have demonstrated good outcomes.^{2,8,9} However, the demand for metal-free restorations resulted in an increasing use of ceramic restorations.⁸ Zirconia-based restorations have become popular due to their excellent mechanical properties and computer-aided manufacturing process.⁷ However, implant-supported zirconia-based restorations had some drawbacks, such as high incidence of porcelain chipping, associated with absence of shock-absorbing periodontal ligaments.¹⁰⁻¹⁴ The load range varies between 17 to 450 N during mastication.¹⁵ Monolithic zirconia restorations, which are partially veneered with a feldspathic porcelain in nonfunctional facial areas, have been recommended to eliminate chipping failures.^{7,16,17} In recent years, the use of implant-supported monolithic zirconia restorations has been considerably increased.^{7,18-22} Complete-arch implant-

supported monolithic zirconia restorations have been associated with short-term clinical success; however, the long-term clinical outcomes are required to validate short-term results.¹⁹

Zirconia is a material that is 10 times harder than titanium, and a review of literature points out that titanium-zirconia connection results in the wear of titanium components.^{17,23,24-26} Chang et al. have reported that monolithic zirconia framework caused deterioration of titanium screw-retained abutments (SRA).¹⁷ As a solution, bonded metal copings to zirconia frameworks have been proposed to provide a metal-to-metal connection, and thus reduce the wear effect of zirconia material.^{17,27}

For the last couple of years, titanium base (Ti-base) abutments have gained a great popularity related to developments in computer-aided manufacturing and computer-aided design (CAD-CAM) dentistry and material science, and the hybrid abutment and hybrid abutment crown concepts have been emerged.^{14,28-33} The hybrid abutment is a customized ceramic abutment cemented to Ti-base abutment, and the hybrid abutment crown is a structure where the abutment and crown are fabricated as 1-piece cemented to the Ti-base abutment and screwed to the implant.³⁴ The hybrid structure allows the achievement of both the mechanical advantage of metal-to-metal connection and the esthetic outcomes of ceramic restorations.³⁴ Recently, the non-engaging titanium-base abutment (N-TiBA) system has been introduced as a novel screw-retained solution for I-FDPs.^{35,36} The non-engaging implant-abutment connection tolerates non-parallel implant angulations and facilitates the insertion of restoration.³⁷

The design of the implant-abutment connection has an important role in the transmission of occlusal stresses.^{36,38,39} Non-engaging implant-abutment connection designs are different for tissue-level and bone-level implant systems. However, limited data is available for evaluating the biomechanical behaviors of these novel prosthetic components.³⁶ The purpose of this research was to examine the biomechanical characteristics of recently introduced tissue-level and bone-level N-TiBA bonded to monolithic zirconia

restorations, in terms of stress distribution in implants, abutments, basal screws, and restoration by using three-dimensional finite element analysis (3D-FEA). The hypothesis was that the tissue-level N-TiBA would result in unfavorable stress distribution in the basal screws.

MATERIAL AND METHODS

The present study was carried out in accordance with the Declaration of Helsinki. This study simulated a 3D finite element model of the maxillary right posterior region with screw-retained, 3-unit I-FDPs. As the FEA studies are in vitro studies based on software simulations, an ethics committee approval was not received. The dimensions of the implants and abutments used in the study are listed in Table 1. The Young moduli and Poisson ratio of each material are listed in Table 2.⁴⁰⁻⁴⁴

The 3D implant and abutment models were created by using scan data of the original components,

TABLE 1: Dimensions of implants and abutments.

Implants			Abutments		
Tissue-level	L	10	Tissue-level	D	5.05
	CD	4.8	N-TiBA	AH	4
	AD	4.1	-	-	-
Bone-level	L	10	Bone-level	D	4.5
	CD	4.1	N-TiBA	AH	3.5
	AD	4.1		GH	-
			Bone-level	D	4.6
			SRA	AH	-
				GH	1

L: length; AD: apical diameter; CD: coronal diameter; D: diameter; AH: abutment height; GH: gingival height; N-TiBA: non-engaging titanium base abutment.

TABLE 2: Young modulus and Poisson ratio of each material.

Material	Young Modulus (GPa)	Poisson Ratio
Cortical bone ⁴⁰	13.7	0.30
Cancellous bone ⁴⁰	1.37	0.30
Titanium-zirconium implant ⁴¹	100	0.30
Titanium abutment ⁴⁰	110	0.35
Titanium screw ⁴⁰	110	0.35
Monolithic zirconia ⁴²	210	0.30
Dual cured resin cement ⁴³	18.6	0.28
Composite resin ⁴⁴	16.6	0.24

listed as follows: a tissue-level titanium-zirconium (Ti-Zr) implant (Roxolid SLActive, Standard Plus, Regular Neck, Straumann AG, Basel, Switzerland); a bone-level Ti-Zr implant (Roxolid SLActive, Regular CrossFit, Straumann AG, Basel, Switzerland); a titanium SRA (RC Screw-retained Abutment, Straumann AG, Basel, Switzerland) with basal and occlusal screw; a titanium coping (Variobase for Bridge/Bar Cylindrical Coping for Screw-retained Abutments Ø 4.6 mm, Straumann AG, Basel, Switzerland); a titanium N-TiBA for tissue level (RN Variobase for Bridge/Bar Cylindrical, Straumann AG, Basel, Switzerland); a titanium N-TiBA for bone-level (RC Variobase for Bridge/Bar Cylindrical, Straumann AG, Basel, Switzerland); and their inner screws. The scan process was conducted on the macro scale by using an optical desktop scanner (Activity 880, Smart Optics Sensortechnik GmbH, Bochum, Germany). The scan data of each component was saved in the standard tessellation language (STL) file format and transferred into 3D modeling software (Rhinoceros v4.0, McNeel Europe Corp., Seattle, WA, USA).

A maxillary right posterior bone structure was modeled using the 3D modeling software. The thickness of the cortical bone was determined to be 1.5 mm.⁴⁵ The cortical bone and cancellous bones were modeled in different colors. In all simulation models, the first implant was placed in the first premolar area, and the second was placed in the first molar area. Six study models were simulated according to a combination of implants, abutments, and crown height.

In model 1 (TL6), the tissue-level implant and N-TiBA models were used. The N-TiBAs were fixed to the implants with 35 Ncm. A maxillary screw-retained 3-unit fixed dental prosthesis (FDP) with a 6 mm of crown height was modeled over the N-TiBAs. A resin cement (Panavia F 2.0, Kuraray Medical Inc, Osaka, Japan) layer 30 µm in thickness was created between the N-TiBAs and restoration with perfect adaptation.^{46,47} In model 2 (TL10), the same protocol was conducted with 10 mm of crown height.

In model 3 (SR6), the bone-level implant, SRA, and titanium coping models were used. The SRAs

were fixed to the implants with 35 Ncm. A maxillary screw-retained 3-unit fixed dental prosthesis (FDP) with a 6 mm crown height was modeled over the titanium copings. A resin cement layer 30 µm in thickness was created between the titanium copings and restoration with perfect adaptation. The restoration bonded to the metal copings was fixed to the basal screws in the SRA by using occlusal screws with 15 Ncm. In model 4 (SR10), the same protocol was conducted with 10 mm of crown height. The M3 and M4 served as control models. The tissue-level SRA models were not included due to lack of titanium metal copings compatible with tissue-level SRA abutment (RN synOcta Abutment, Straumann AG, Basel, Switzerland).

In model 5 (BL6), the bone-level implant and N-TiBA models were used. The N-TiBAs were fixed to

the implants with 35 Ncm. A maxillary screw-retained 3-unit fixed dental prosthesis (FDP) with a 6 mm crown height was modeled over the N-TiBAs, and a resin cement layer 30 µm in thickness was created between the N-TiBAs and restoration with perfect adaptation. In model 6 (BL10), the same protocol was conducted with 10 mm of crown height. In all restoration models, the screw access holes were filled with a composite layer from the top of abutment to occlusal surface. All study models are presented in Figure 1.

All 3D models were meshed with 10-node tetrahedron quadratic elements by using meshing software (VRMesh Studio, VirtualGrid Inc, Bellevue City, WA, USA), and meshed models were transferred to the FEA software (Algor Fempro, Algor Inc, Pittsburgh, PA, USA) for stress analyses. The final mod-

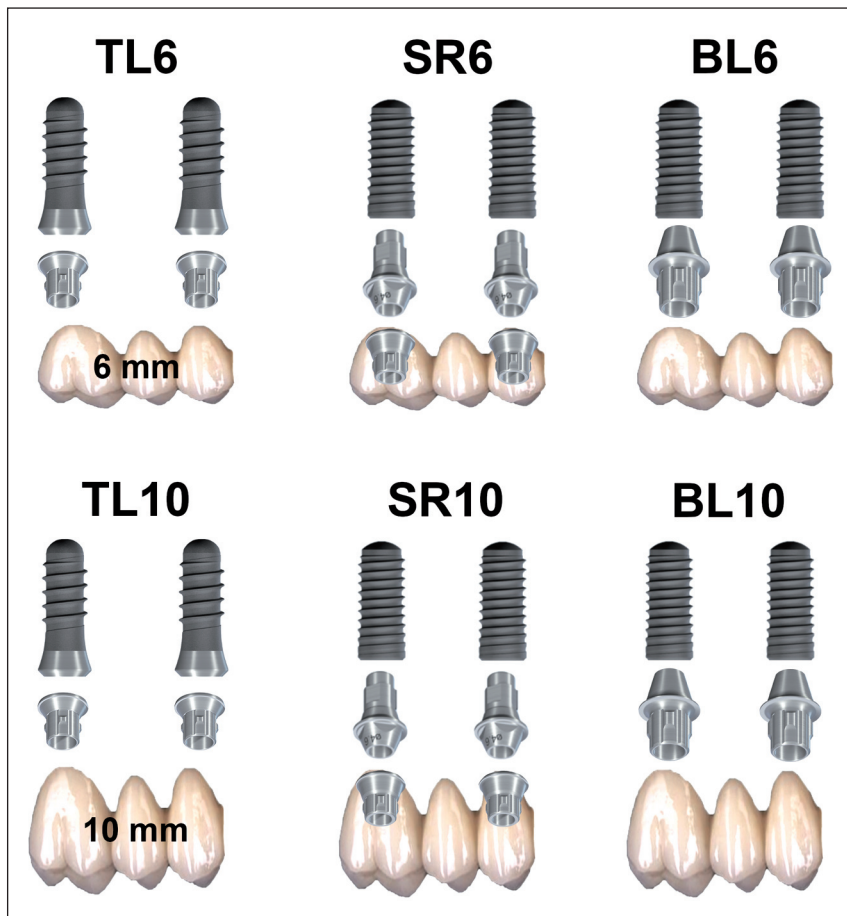


FIGURE 1: Study models. **TL6:** Tissue-level and non-engaging titanium base abutment with 6 mm crown height; **TL10:** Tissue-level and non-engaging titanium base abutment with 10 mm crown height; **SR6:** Bone-level and screw-retained abutment with 6 mm crown height; **SR10:** Bone-level and screw-retained abutment with 10 mm crown height; **BL6:** Bone-level and non-engaging titanium base abutment with 6 mm crown height; **BL10:** Bone-level and non-engaging titanium base abutment with 10 mm crown height.

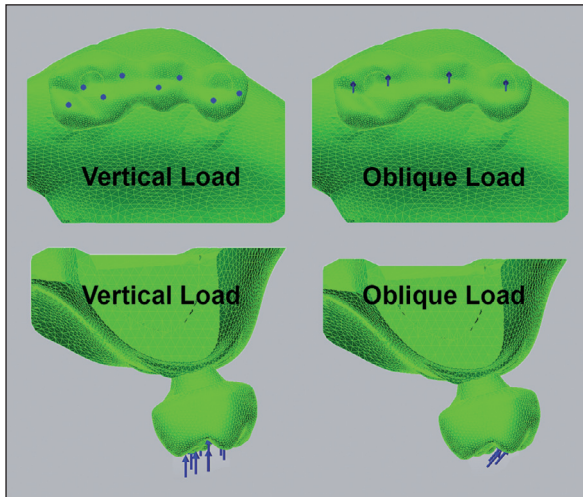


FIGURE 2: Loading directions.

els had a total of 97,028 nodes and 459,819 elements for the TL6; 98,144 nodes and 460,343 elements for the TL10; 144,640 nodes and 712,420 elements for the SR6; 146,465 nodes and 718,052 elements for the SR10; 116,169 nodes and 555,540 elements for the BL6; and 119,570 nodes and 570,262 elements for the BL10. All materials were considered linear, elastic, homogenous, and isotropic. A 100% osseointegration was simulated between the implants and bone, and gingiva was ignored. The boundary conditions were determined as no movement in each axis at the mesial and distal external borders. The restoration material was determined as monolithic zirconia.

In each model, 200 N of vertical load (50 N to 4 centric points on the molar and 100 N to 2 centric points on the premolars), and 100 N of oblique load (50 N to each buccal cusp on the molar and 100 N to buccal cusp on the premolars) were applied to the palatal incline of the buccal cusps at 45 degrees (Figure 2).^{41,48} Simultaneous and equal vertical and oblique loads were applied to each premolar and molar tooth.⁴⁹ The von Mises stress (vMS) analysis was used to evaluate stress distributions in the implants, abutments, basal screws, and restoration.⁵⁰

RESULTS

The vMS analysis results are shown in Table 3. The oblique load generated more stress in the implants, abutments, basal screws, and restorations. The in-

crease in the crown height did not have a significant impact on stress concentrations under vertical loading but did so on the stress concentrations under oblique loading.

In the implant models, the vMS were concentrated in the cervical region, where the implant and abutment are connected (Figure 3). The TL6 and TL10 exhibited higher vMS values in the cervical region than in the other FEA models.

In the abutment models, the TL6 and TL10 exhibited the lowest vMS values than in the other FEA models. As in the implant models, the vMS were concentrated in the implant connection area of the abutments (Figure 4). The highest vMS values in the abutment were obtained from the BL6 and BL10.

In the basal screw models, the vMS were concentrated in the coronal shank region, where the screw and abutment are in contact in most of the models (Figure 5). The BL6 and BL10 exhibited the highest vMS stress values under both vertical and oblique loading. The SR6 and SR10 exhibited the lowest vMS values under vertical loading, whereas the TL6 and TL10 exhibited the lowest vMS values under oblique loading.

In the restoration models, the vMS were concentrated in the cervical region of restorations facing the abutments (Figure 6). The BL6 and BL10 exhibited the highest vMS stress values in the cervical region of restorations.

DISCUSSION

In the present study, the tissue-level and bone-level N-TiBA designs were evaluated in terms of their biomechanical effects on stress distribution in implants and prosthetic components. The main design difference between the 2 N-TiBAs was that the tissue-level design had a shorter internal non-engaging connection area than the bone-level. This important difference formed the basis of the study hypothesis. According to the vMS analysis results, the basal screws in the tissue-level N-TiBAs exhibited low stress values within the structure. Therefore, the hypothesis that the tissue-level N-TiBA would result in unfavorable stress distribution in the basal screws was rejected.



FIGURE 3: von Mises stresses in implant models. **TL6:** Tissue-level and non-engaging titanium base abutment with 6 mm crown height; **TL10:** Tissue-level and non-engaging titanium base abutment with 10 mm crown height; **SR6:** Bone-level and screw-retained abutment with 6 mm crown height; **SR10:** Bone-level and screw-retained abutment with 10 mm crown height; **BL6:** Bone-level and non-engaging titanium base abutment with 6 mm crown height; **BL10:** Bone-level and non-engaging titanium base abutment with 10 mm crown height.

The vMS values are defined as the point where the deformation begins for ductile materials, such as implants. A failure may occur when the vMS values exceed the yield strength of an implant (550 MPa).⁵⁰ In the present study, no implant model exhibited a vMS value >550 MPa; however, higher stress values were observed in the bone-level N-TiBAs under oblique loading. The loading conditions in the present study were set to 200 N vertically and 100 N obliquely, and higher occlusal loads could be observed in the oral cavity.¹⁵ The increase in the intensity and incidence of masticatory loads may result in implant failure in long-term use.

In the present study, the intensity of loading conditions was not equal because total vertical and oblique loads were divided differently.⁴⁸ The vertical

load received by 2 centric points in the premolars and 4 centric points in the molar, and the oblique load received by only buccal cusps.⁴⁸ Despite the lower intensity, the oblique load resulted in higher stress concentrations in the implants and prosthetic components. Similar results have been found in previous studies.^{13,39} The intensity of masticatory loads is variable, especially in the molar region.¹⁵ Therefore, the presence of optimum occlusal contacts is essential for implant-supported prostheses. Any occlusal interference must be eliminated in order to prevent unfavorable stresses.

The increase in the crown height has the potential to elevate the mechanical load on the implants because of the alteration in the implant-crown ratio.⁵¹ de Moraes et al. reported that this increase

TABLE 3: von Mises stress analysis results.

N/mm ² (MPa)	Models	Premolar		Molar	
		Vertical Load	Oblique Load	Vertical Load	Oblique Load
Implant	TL6	127	217	109	194
	TL10	131	284	108	265
	SR6	63	85	76	110
	SR10	63	105	77	136
	BL6	60	79	62	89
	BL10	59	98	63	110
Abutment	TL6	160	221	111	179
	TL10	172	336	119	251
	SR6	199	376	160	361
	SR10	202	505	165	504
	BL6	313	632	278	613
	BL10	316	863	284	847
Basal screw	TL6	59	68	38	65
	TL10	60	82	39	82
	SR6	40	126	40	147
	SR10	41	198	51	175
	BL6	85	243	80	249
	BL10	86	342	83	351
Restoration	TL6	40	70	19	29
	TL10	47	102	40	63
	SR6	41	47	27	52
	SR10	46	71	33	87
	BL6	118	169	138	280
	BL10	93	204	64	202

TL6: Tissue-level and non-engaging titanium base abutment with 6 mm crown height; TL10: Tissue-level and non-engaging titanium base abutment with 10 mm crown height; SR6: Bone-level and screw-retained abutment with 6 mm crown height; SR10: Bone-level and screw-retained abutment with 10 mm crown height; BL6: Bone-level and non-engaging titanium base abutment with 6 mm crown height; BL10: Bone-level and non-engaging titanium base abutment with 10 mm crown height.

enhances the stress concentration at the implant-bone interface mainly under oblique loading.⁵² The results of the present study were consistent with this finding. The increase in the crown height did not cause a considerable rise in stress values under vertical loading, while a significant elevation was observed under oblique loading.

The results of the present study showed that vMS was concentrated in the implant-abutment connection area for both the implants and abutments. Similarly, the same stress pattern was observed in the shank region of basal screws, where the screw and abutment meet. This is a natural result that occurs when 2 materials are in contact. As one of the materials is loaded, the stresses concentrate at the connection area.⁵³

As mentioned before, the abutment design plays a significant role in stress transfer.^{36,38,39} The present study theorized that the tissue-level N-TiBA may lead to excessive stress concentrations in the basal screws due to the short internal non-engaging connection area. Instead, the results revealed that tissue-level N-TiBAs generated more stress in the implants rather than in the basal screws. Moreover, the tissue-level N-TiBAs exhibited less stress within the structure. The cervical region of the tissue-level N-TiBA seats onto the implant platform and the length of internal connection area is shorter than in bone-level abutments, which have a platform switching design. The direct contact with the implant platform may lead to most of the stresses being transferred to the implant rather being absorbed, and this may explain

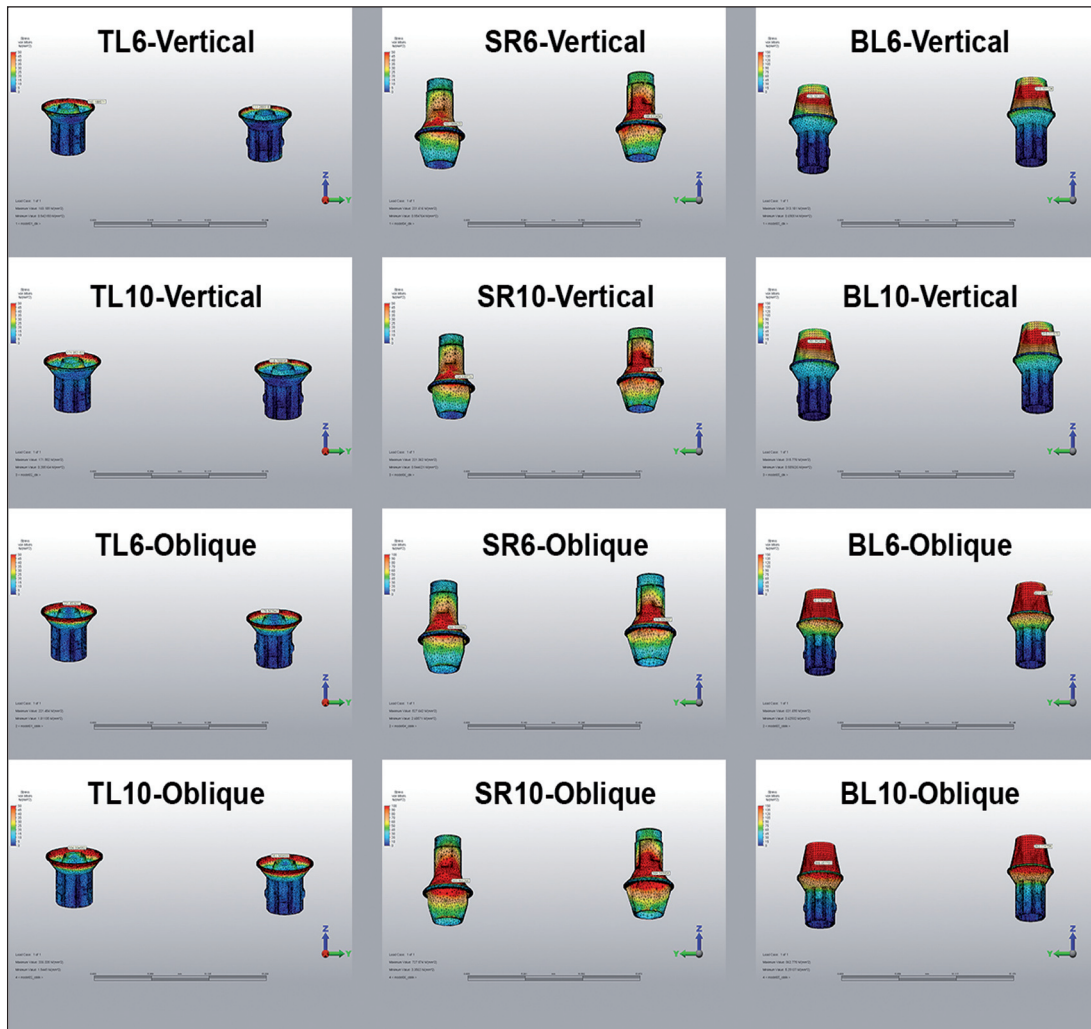


FIGURE 4: von Mises stresses in abutment models. TL6: Tissue-level and non-engaging titanium base abutment with 6 mm crown height; TL10: Tissue-level and non-engaging titanium base abutment with 10 mm crown height; SR6: Bone-level and screw-retained abutment with 6 mm crown height; SR10: Bone-level and screw-retained abutment with 10 mm crown height; BL6: Bone-level and non-engaging titanium base abutment with 6 mm crown height; BL10: Bone-level and non-engaging titanium base abutment with 10 mm crown height.

the high stress values in the cervical region of tissue-level implants and the low stress values in the basal screws.

Furthermore, the highest stress values in the abutments, basal screws, and restorations were observed in the bone-level N-TiBA models. Engaging abutments have insertion grooves that prevent the abutment from rotational movements, especially under oblique loading.³⁶ Conversely, non-engaging abutments do not have insertion grooves to facilitate the path of the I-FDPs.³⁷ The non-engaging connection may lead to micromovements of the abutment, and this may result in extra stress concentration

within the structure and the other components that are in contact. Despite the non-engaging connection, the same stress pattern was not observed in the tissue-level N-TiBA. It is thought that the connection with the tissue-level implant platform may minimize the micromovements.

The stress analysis showed that the basal screw in the bone-level SRA models exhibited different biomechanical behaviors under vertical and oblique loading. High stress values were observed under oblique loading, while low stress values occurred under vertical loading. When the 2 components are connected together by a screw, this connection is de-

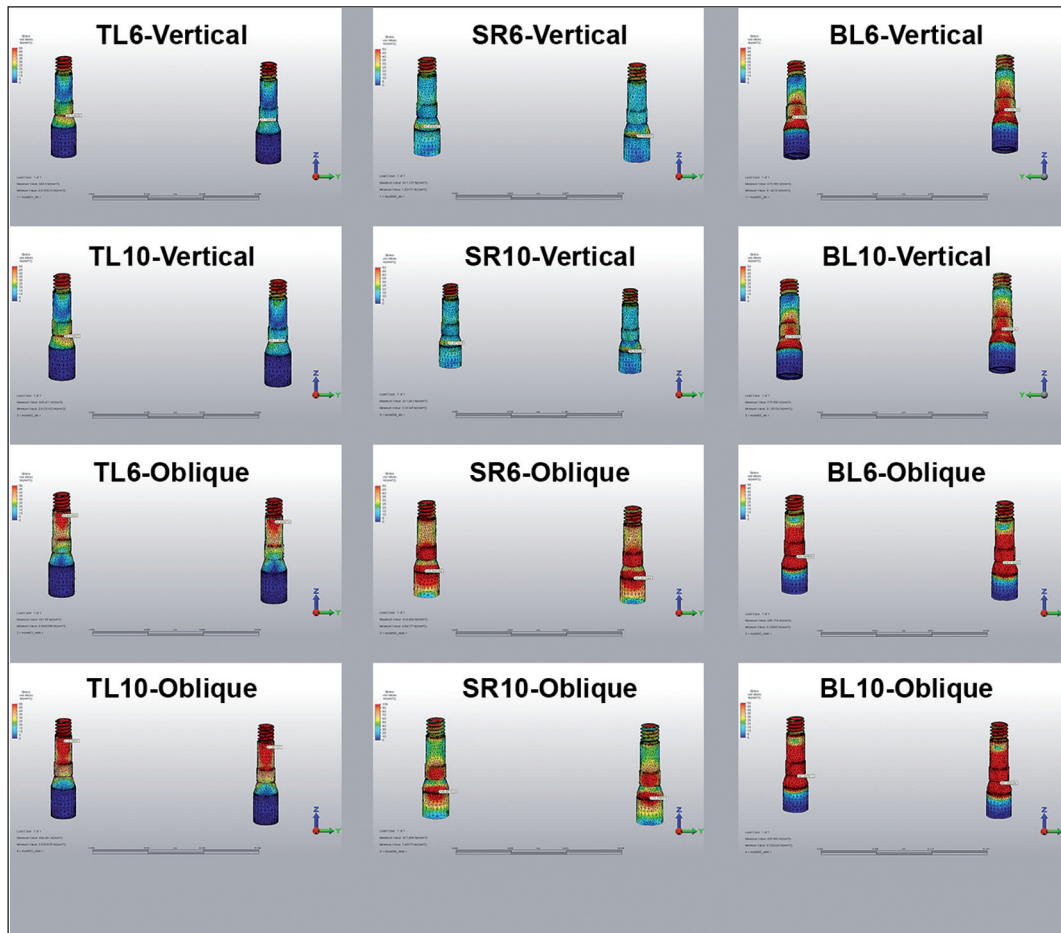


FIGURE 5: von Mises stresses in basal screw models. **TL6:** Tissue-level and non-engaging titanium base abutment with 6 mm crown height; **TL10:** Tissue-level and non-engaging titanium base abutment with 10 mm crown height; **SR6:** Bone-level and screw-retained abutment with 6 mm crown height; **SR10:** Bone-level and screw-retained abutment with 10 mm crown height; **BL6:** Bone-level and non-engaging titanium base abutment with 6 mm crown height; **BL10:** Bone-level and non-engaging titanium base abutment with 10 mm crown height.

defined as screw joint.⁵⁴ The bone-level SRA system used in the present study includes 2 screw joints. The SRA is fixed to the implant with the basal screw while the restoration is fixed to the basal screw with occlusal screws. It is thought that this double-joint system may not be as stable as single-screw systems under oblique loading and may lead to high stress values in the coronal shank region of the basal screws.

In the present study, only 3-unit I-FDPs were utilized, and the stress distribution was evaluated in a standardized bone density. Different biomechanical behaviors may be observed in complete-arch I-FDPs and in various bone densities. Moreover, only a single type of implant system

was evaluated in vitro. Clinical follow-up studies are required to provide more comprehensive results.

CONCLUSION

Within the limitations of this study, the following conclusions were drawn:

1. Oblique loads resulted in higher stress values than vertical loads.
2. The implant-abutment connection affected the stress distribution.
3. The tissue-level implants exhibited higher stress values in the cervical region than bone-level implants.

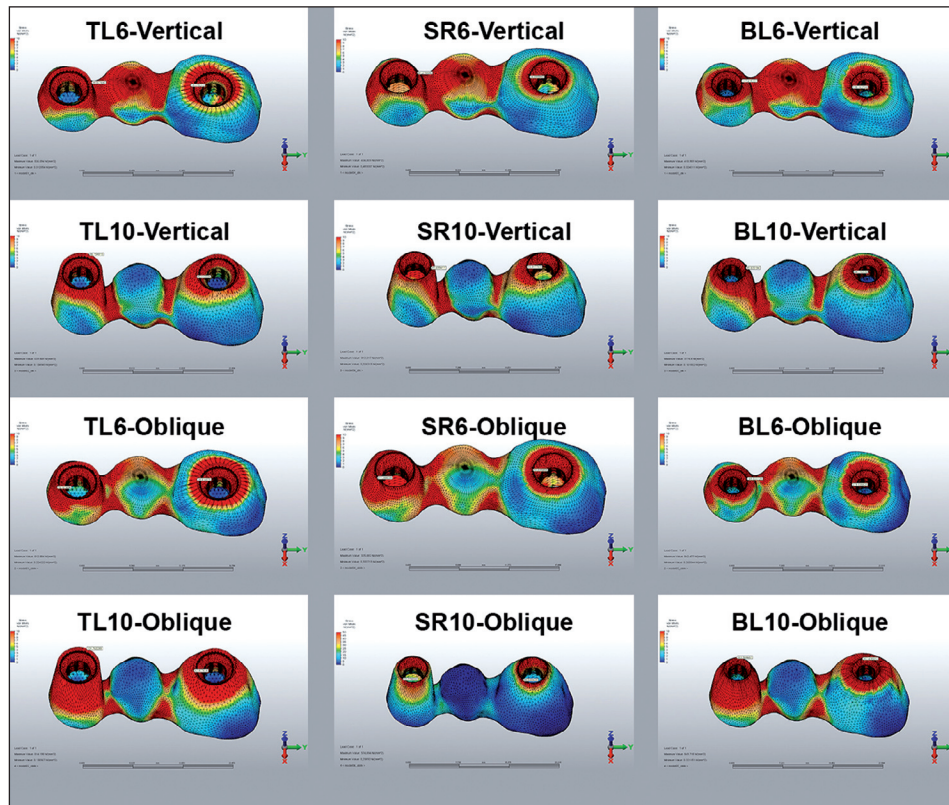


FIGURE 6: von Mises stresses in restoration models. **TL6:** Tissue-level and non-engaging titanium base abutment with 6 mm crown height; **TL10:** Tissue-level and non-engaging titanium base abutment with 10 mm crown height; **SR6:** Bone-level and screw-retained abutment with 6 mm crown height; **SR10:** Bone-level and screw-retained abutment with 10 mm crown height; **BL6:** Bone-level and non-engaging titanium base abutment with 6 mm crown height; **BL10:** Bone-level and non-engaging titanium base abutment with 10 mm crown height.

4. The tissue-level N-TiBAs exhibited lower stress values in the implant connection area compared to bone-level abutments.

Source of Finance

During this study, no financial or spiritual support was received neither from any pharmaceutical company that has a direct connection with the research subject, nor from a company that provides or produces medical instruments and materials which may negatively affect the evaluation process of this study.

Conflict of Interest

No conflicts of interest between the authors and / or family members of the scientific and medical committee members or members of the potential conflicts of interest, counseling, expertise, working conditions, share holding and similar situations in any firm.

Authorship Contributions

All authors contributed equally while this study preparing.

REFERENCES

1. Silva GC, Comacchia TM, de Magalhães CS, Bueno AC, Moreira AN. Biomechanical evaluation of screw-and cement-retained implant-supported prostheses: a nonlinear finite element analysis. *J Prosthet Dent.* 2014;112(6):1479-88. [\[Crossref\]](#) [\[PubMed\]](#)
2. Wittneben JG, Millen C, Brägger U. Clinical performance of screw-versus cement-retained fixed implant-supported reconstructions-a systematic review. *Int J Oral Maxillofac Implants.* 2014;29 Suppl:84-98. [\[Crossref\]](#) [\[PubMed\]](#)
3. Sailer I, Muhlemann S, Zwahlen M, Hämmerle CH, Schneider D. Cemented and screw-retained implant reconstructions: a systematic review of the survival and complication rates. *Clin Oral Implants Res.* 2012;23 Suppl 6:163-201. [\[Crossref\]](#) [\[PubMed\]](#)
4. Lemos CA, de Souza Batista VE, Almeida DA, Santiago Júnior JF, Verri FR, Pellizzer EP. Evaluation of cement-retained versus screw-retained implant-supported restorations for marginal bone loss: a systematic review and meta-analysis. *J Prosthet Dent.* 2016;115(4): 419-27. [\[Crossref\]](#) [\[PubMed\]](#)

5. Wilson TG Jr. The positive relationship between excess cement and peri-implant disease: a prospective clinical endoscopic study. *J Periodontol.* 2009;80(9):1388-92. [[Crossref](#)] [[PubMed](#)]
6. Korsch M, Obst U, Walther W. Cement-associated peri-implantitis: a retrospective clinical observational study of fixed implant-supported restorations using a methacrylate cement. *Clin Oral Implants Res.* 2014;25(7):797-802. [[Crossref](#)] [[PubMed](#)]
7. Venezia P, Torsello F, Cavalcanti R, D'Amato S. Retrospective analysis of 26 complete-arch implant-supported monolithic zirconia prostheses with feldspathic porcelain veneering limited to the facial surface. *J Prosthet Dent.* 2015;114(4):506-12. [[Crossref](#)] [[PubMed](#)]
8. Worni A, Kolgeci L, Rentsch-Kollar A, Katsoulis J, Mericske-Stern R. Zirconia-based screw-retained prostheses supported by implants: a retrospective study on technical complications and failures. *Clin Implant Dent Relat Res.* 2015;17(6):1073-81. [[Crossref](#)] [[PubMed](#)]
9. Mehra M, Mahidi F. Complete mouth implant rehabilitation with a zirconia ceramic system: a clinical report. *J Prosthet Dent.* 2014;112(1):1-4. [[Crossref](#)] [[PubMed](#)]
10. Konstantinidis IK, Jacoby S, Rädcl M, Böning K. Prospective evaluation of zirconia based tooth-and implant-supported fixed dental prostheses: 3-year results. *J Dent.* 2015;43(1):87-93. [[Crossref](#)] [[PubMed](#)]
11. Guess PC, Att W, Strub JR. Zirconia in fixed implant prosthodontics. *Clin Implant Dent Relat Res.* 2012;14(5):633-45. [[Crossref](#)] [[PubMed](#)]
12. de Kok P, Kleverlaan CJ, de Jager N, Kuijs R, Feilzer AJ. Mechanical performance of implant-supported posterior crowns. *J Prosthet Dent.* 2015;114(1):59-66. [[Crossref](#)] [[PubMed](#)]
13. Kaleli N, Sarac D, Külünk S, Öztürk Ö. Effect of different restorative crown and customized abutment materials on stress distribution in single implants and peripheral bone: a three-dimensional finite element analysis study. *J Prosthet Dent.* 2018;119(3):437-45. [[Crossref](#)] [[PubMed](#)]
14. Elshiyab SH, Nawafleh N, Walsh L, George R. Fracture resistance and survival of implant-supported, zirconia-based hybrid-abutment crowns: influence of aging and crown structure. *J Investig Clin Dent.* 2018;9(4):e12355. [[Crossref](#)] [[PubMed](#)]
15. Morneburg TR, Pröschel PA. Measurement of masticatory forces and implant loads: a methodologic clinical study. *Int J Prosthodont.* 2002;15(1):20-7.
16. Guess PC, Schultheis S, Bonfante EA, Coelho PG, Ferencz JL, Silva NR. All-ceramic systems: laboratory and clinical performance. *Dent Clin North Am.* 2011;55(2):333-52. [[Crossref](#)] [[PubMed](#)]
17. Chang JS, Ji W, Choi CH, Kim S. Catastrophic failure of a monolithic zirconia prosthesis. *J Prosthet Dent.* 2015;113(2):86-90. [[Crossref](#)] [[PubMed](#)]
18. Rojas-Vizcaya F. Full zirconia fixed detachable implant-retained restorations manufactured from monolithic zirconia: clinical report after two years in service. *J Prosthodont.* 2011;20(7):570-6. [[Crossref](#)] [[PubMed](#)]
19. Abdulmajeed AA, Lim KG, Nārhi TO, Cooper LF. Complete-arch implant-supported monolithic zirconia fixed dental prostheses: a systematic review. *J Prosthet Dent.* 2016;115(6):672-7.e1. [[Crossref](#)] [[PubMed](#)]
20. Cheng CW, Chien CH, Chen CJ, Pappaspyridakos P. Complete-mouth implant rehabilitation with modified monolithic zirconia implant-supported fixed dental prostheses and an immediate-loading protocol: a clinical report. *J Prosthet Dent.* 2013;109(6):347-52. [[Crossref](#)]
21. Cardelli P, Manobianco FP, Serafini N, Murrura G, Beuer F. Full-arch, implant-supported monolithic zirconia rehabilitations: pilot clinical evaluation of wear against natural or composite teeth. *J Prosthodont.* 2016;25(8):629-33. [[Crossref](#)] [[PubMed](#)]
22. Altarawneh S, Limmer B, Reside GJ, Cooper L. Dual jaw treatment of edentulism using implant-supported monolithic zirconia fixed prostheses. *J Esthet Restor Dent.* 2015;27(2):63-70. [[Crossref](#)] [[PubMed](#)]
23. Brodbeck U. The ZiReal post: a new ceramic implant abutment. *J Esthet Restor Dent.* 2003;15(1):10-24. [[Crossref](#)] [[PubMed](#)]
24. Stimmelmayer M, Edelhoff D, Güth JF, Erdelt K, Happe A, Beuer F. Wear at the titanium-titanium and the titanium-zirconia implant-abutment interface: a comparative in vitro study. *Dent Mater.* 2012;28(12):1215-20. [[Crossref](#)] [[PubMed](#)]
25. Klotz MW, Taylor TD, Goldberg AJ. Wear at the titanium-zirconia implant-abutment interface: a pilot study. *Int J Oral Maxillofac Implants.* 2011;26(5):970-5.
26. Taylor TD, Klotz MW, Lawton RA. Titanium tattooing associated with zirconia implant abutments: a clinical report of two cases. *Int J Oral Maxillofac Implants.* 2014;29(4):958-60. [[Crossref](#)] [[PubMed](#)]
27. Rojas Vizcaya F. Retrospective 2-to 7-year follow-up study of 20 double full-arch implant-supported monolithic zirconia fixed prostheses: measurements and recommendations for optimal design. *J Prosthodont.* 2018;27(6):501-8. [[Crossref](#)] [[PubMed](#)]
28. Kurbad A, Kurbad S. CAD/CAM-based implant abutments. *Int J Comput Dent.* 2013;16(2):125-41.
29. Kim JS, Raigrodski AJ, Flinn BD, Rubenstein JE, Chung KH, Mancl LA. In vitro assessment of three types of zirconia implant abutments under static load. *J Prosthet Dent.* 2013;109(4):255-63. [[Crossref](#)]
30. Elshiyab SH, Nawafleh N, Öchsner A, George R. Fracture resistance of implant-supported monolithic crowns cemented to zirconia hybrid-abutments: zirconia-based crowns vs. lithium disilicate crowns. *J Adv Prosthodont.* 2018;10(1):65-72. [[Crossref](#)] [[PubMed](#)] [[PMC](#)]
31. Zeller S, Guichet D, Kontogiorgos E, Nagy WW. Accuracy of three digital workflows for implant abutment and crown fabrication using a digital measuring technique. *J Prosthet Dent.* 2019;121(2):276-84. [[Crossref](#)] [[PubMed](#)]
32. Kelly JR, Rungruangnunt P. Fatigue behavior of computer-aided design/computer-assisted manufacture ceramic abutments as a function of design and ceramics processing. *Int J Oral Maxillofac Implants.* 2016;31(3):601-9. [[Crossref](#)] [[PubMed](#)]
33. Selz CF, Vuck A, Guess PC. Full-mouth rehabilitation with monolithic CAD/CAM-fabricated hybrid and all-ceramic materials: a case report and 3-year follow up. *Quintessence Int.* 2016;47(2):115-21.
34. Elsayed A, Wille S, Al-Akhali M, Kern M. Effect of fatigue loading on the fracture strength and failure mode of lithium disilicate and zirconia implant abutments. *Clin Oral Implants Res.* 2018;29(1):20-7. [[Crossref](#)] [[PubMed](#)]
35. Worni A, Katsoulis J, Kolgeci L, Worni M, Mericske-Stern R. Monolithic zirconia reconstructions supported by teeth and implants: 1-to 3-year results of a case series. *Quintessence Int.* 2017;48(6):459-67.
36. Epprecht A, Zeltner M, Benic G, Özcan M. A strain gauge analysis comparing 4-unit veneered zirconium dioxide implant-borne fixed dental prosthesis on engaging and non-engaging abutments before and after torque application. *Clin Exp Dent Res.* 2018;4(1):13-8. [[Crossref](#)] [[PubMed](#)] [[PMC](#)]
37. Schoenbaum TR, Stevenson RG, Balinghasay E. The hemi-engaging fixed dental implant prosthesis: a technique for improved stability and handling. *J Prosthet Dent.* 2018;120(1):17-9. [[Crossref](#)] [[PubMed](#)]
38. Saidin S, Abdul Kadir MR, Sulaiman E, Ebu Kasim NH. Effects of different implant-abutment connections on micromotion and stress distribution: prediction of microgap formation. *J Dent.* 2012;40(6):467-74. [[Crossref](#)] [[PubMed](#)]
39. Takahashi JM, Dayrell AC, Consani RL, de Aruda Nóbilo MA, Henriques GE, Mesquita MF. Stress evaluation of implant-abutment connections under different loading conditions: a 3D finite element study. *J Oral Implantol.* 2015;41(2):133-7. [[Crossref](#)] [[PubMed](#)]

40. Eskitascioglu G, Usumez A, Sevimay M, Soykan E, Unsal E. The influence of occlusal loading location on stresses transferred to implant-supported prostheses and supporting bone: a three-dimensional finite element study. *J Prosthet Dent.* 2004;91(2):144-50. [[Crossref](#)] [[PubMed](#)]
41. Cinel S, Celik E, Sagirkaya E, Sahin O. Experimental evaluation of stress distribution with narrow diameter implants: a finite element analysis. *J Prosthet Dent.* 2018;119(3):417-25. [[Crossref](#)] [[PubMed](#)]
42. Franco-Tabares S, Stenport VF, Hjalmarsson L, Johansson CB. Limited effect of cement material on stress distribution of a monolithic translucent zirconia crown: a three-dimensional finite element analysis. *Int J Prosthodont.* 2018;31(1):67-70. [[Crossref](#)] [[PubMed](#)]
43. Lanza A, Aversa R, Rengo S, Apicella D, Apicella A. 3D FEA of cemented steel, glass and carbon posts in a maxillary incisor. *Dent Mater.* 2005;21(8):709-15. [[Crossref](#)] [[PubMed](#)]
44. Soares PV, Santos-Filho PCF, Queiroz EC, Araújo TC, Campos RE, Araújo CA, et al. Fracture resistance and stress distribution in endodontically treated maxillary premolars restored with composite resin. *J Prosthodont.* 2008;17(2):114-9. [[Crossref](#)] [[PubMed](#)]
45. Katranji A, Misch K, Wang HL. Cortical bone thickness in dentate and edentulous human cadavers. *J Periodontol.* 2007;78(5):874-8. [[Crossref](#)] [[PubMed](#)]
46. Wu JC, Wilson PR. Optimal cement space for resin luting cements. *Int J Prosthodont.* 1994;7(3):209-15.
47. Kious AR, Roberts HW, Brackett WW. Film thicknesses of recently introduced luting cements. *J Prosthet Dent.* 2009;101(3):189-92. [[Crossref](#)]
48. de Faria Almeida DA, Pellizzer EP, Verri FR, Santiago Jr JF, de Carvalho PSP. Influence of tapered and external hexagon connections on bone stresses around tilted dental implants: three-dimensional finite element method with statistical analysis. *J Periodontol.* 2014;85(2):261-9. [[Crossref](#)] [[PubMed](#)]
49. Lin CL, Wang JC, Chang SH, Chen ST. Evaluation of stress induced by implant type, number of splinted teeth, and variations in periodontal support in tooth-implant-supported fixed partial dentures: a non-linear finite element analysis. *J Periodontol.* 2010;81(1):121-30. [[Crossref](#)] [[PubMed](#)]
50. İplikçioğlu H, Akça K. Comparative evaluation of the effect of diameter, length and number of implants supporting three-unit fixed partial prostheses on stress distribution in the bone. *J Dent.* 2002;30(1):41-6. [[Crossref](#)]
51. Nissan J, Ghelfan O, Gross O, Priel I, Gross M, Chaushu G. The effect of crown/implant ratio and crown height space on stress distribution in unsplinted implant supporting restorations. *J Oral Maxillofac Surg.* 2011;69(7):1934-9. [[Crossref](#)] [[PubMed](#)]
52. de Moraes SL, Verri FR, Junior JF Jr, Almeida DA, de Mello CC, Pellizzer EP. A 3-D finite element study of the influence of crown-implant ratio on stress distribution. *Braz Dent J.* 2013;24(6):635-41. [[Crossref](#)] [[PubMed](#)]
53. Nishioka RS, de Vasconcelos LG, Jórias RP, Rode Sde M. Load-application devices: a comparative strain gauge analysis. *Braz Dent J.* 2015;26(3):258-62. [[Crossref](#)] [[PubMed](#)]
54. Alkan I, Sertgöz A, Ekici B. Influence of occlusal forces on stress distribution in preloaded dental implant screws. *J Prosthet Dent.* 2004;91(4):319-25. [[Crossref](#)] [[PubMed](#)]